Analysis of the acoustic signals backscattered by a tube using the time-frequency representations

Mustapha Laaboubi[a], Elhoucien Aassif[a], Rachid Latif[b], Gerard Maze[c], Dominique Decultot[d], Ali Moudden[a] and Abdelilah Dariouchy[e]

[a]Ibn Zohr University, FS Agadir, 80000 Agadir, Morocco
[b]ESSI - ENSA, BP 1136, Ibn Zohr University, 80000 Agadir, Morocco
[c]LAUE, Université du Havre, Place Robert Schuman, F-76610 Le Havre, France
[d]LOMC FRE 3102 CNRS Groupes Ondes Acoustiques, Université du Havre (IUT), Place Robert Schuman, 76610 Le Havre, France
[e]LMTI, univirsté ibn zohr Faculté des Sciences LMTI bp 8106, 80000 Agadir, Morocco
laaboubi@gmail.com

The normal excitation of a tube immersed in water by the acoustic plane wave permits the generation of circumferential waves inside the shell and around the shell-water interface. These circumferential waves, standing form stationary waves on the circumference of the tube for some frequencies. These stationary waves, constituting resonances of the tube which are perfectly visibles on the backscattered spectrum. Moreover, the studies carried out on the diffusion of a plane acoustic wave by target were based primarily on the use of the monodimensional methods (Temporal domain and/or frequencial domain). To exceed the disadvantages of these methods, in this work, we used the time-frequency representations such as the Short-Term Fourier Transform (STFT), Wigner-Ville Distribution (WVD) and Wavelet Transform method. These representations are applied to a theoretical signal backscattered by a tube. From the time-frequency images obtained we have visualized the circumferential waves dispersion (S0, A1, S1,…) and identified these different waves. This analysis permits to compare between these time-frequency representations. And also we have compared between the cut-off frequencies of circumferential waves obtained from these representations and those computed by the proper modes theory of the vibration.

1 Introduction

The study of the acoustic diffusion by targets, of simple geometrical form, was the subject of many works [8,12]. Among the objectives of this work is to try to understand the origin of the circumferential waves and the manner of being propagated around a tube.

The majority of the studies of analysis of the acoustic pressure backscattered by targets immersed in water were based primarily on the use of the monodimensional methods (temporal and spectral analysis). These representations present limitations which make them unadapted to study the dispersion of the circumferential waves contained in a signal backscattered by a target. To exceed these limitations, two-dimensional time-frequency representations are implemented [3,4,11]. They take into account the time and frequency parameters. The time-frequency representations used in this paper are the Spectrgram, the Wavelet Transform and the Wigner-Ville Distribution [1,2]. The signal analysed by these representations is an acoustic signal backscattered by a copper tube with radius ratio b/a = 0.95 (*a* is the external radius, and *b* the internal radius). The aim of this study is to visualise the frequential evolution versus the time of the circumferential waves and to identify them (*S0*, *A1*, *S1*, ...).

2 Complex backscattering pressure by a cylindrical shell

The scattering of an infinite plane wave by a cylindrical shell with a radius ratio b/a is investigated through the solution of the wave equation and the associated boundary conditions [17].

The complex backscattering pressure P_{scat} by a tube in a far field is the summation of the normal modes which take into account the effects of the incident wave [17,19], the reflective wave ①, circumferential waves in the shell ② (whispering gallery waves, Rayleigh wave) and interface Scholte wave (A) ③ connected to the geometry of the object Fig.1. For the circumferential waves, it is necessary to distinguish between the symmetric waves (S0, S1, S2,…) and the antisymmetric waves (A0, A1, A2,…).

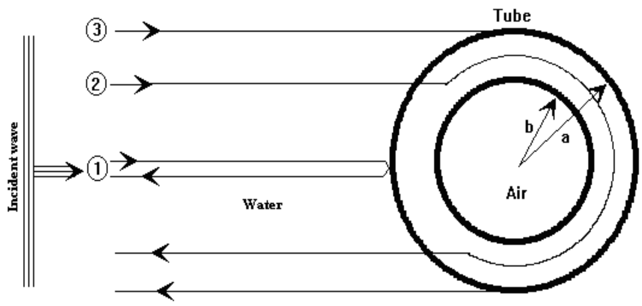

.Fig.1 Mechanisms of the echos formation

The general form of the scattered complex pressure field in a plan perpendicular to the z-axis can be expressed as [17,18]:

$$P_{scat}(\omega) = P_0 \frac{1-i}{\sqrt{\pi k r}} e^{i(ka-\omega t)} \sum_{n=0}^{\infty} \varepsilon_n \frac{D_n^1(\omega)}{D_n(\omega)} \cos(n\theta) \quad (1)$$

Where ω is the angular frequency, $k=\omega/c$ is the wave number with respect to the wave velocity in the external fluid (C), P_0 is the amplitude of the incident plane wave, $D_n^1(\omega)$ and $D_n(\omega)$ are determinants computed from the boundary conditions of the problem (continuity of stress and displacement on the two interfaces), εn is the Neumann coefficient ($\varepsilon_n = 1$ if n=0 and $\varepsilon_n = 2$ if $n \neq 0$) and r is the distance between the z-axis of the tube and the point where the pressure is calculated. The complex backscattering pressure computed in a far field is obtained for $\theta = \pi$ as a function of the dimensionless frequency *k.a* (Fig.2a) which is given by the relation:

$$k.a = \frac{2\pi \nu a}{C} \quad (2)$$

where ν is the wave frequency in Hz.

The resonance spectrum (Fig. 2b) is obtained in three operations:

- the time signal is computed with the Inverse Fourier transform of the calculated backscattered complex pressure (Fig.2a).
- the specular echo (Fig. 2c) which is related to the reflexion on the outer surface of the cylindrical shell is suppressed and replaced by zeros with a computer.
- a Fourier transform is applied to this new time signal to obtain the resonance spectrum (Fig.2b). In theoritical study this resonance spectrum is obtained suppressing the rigid or soft background.

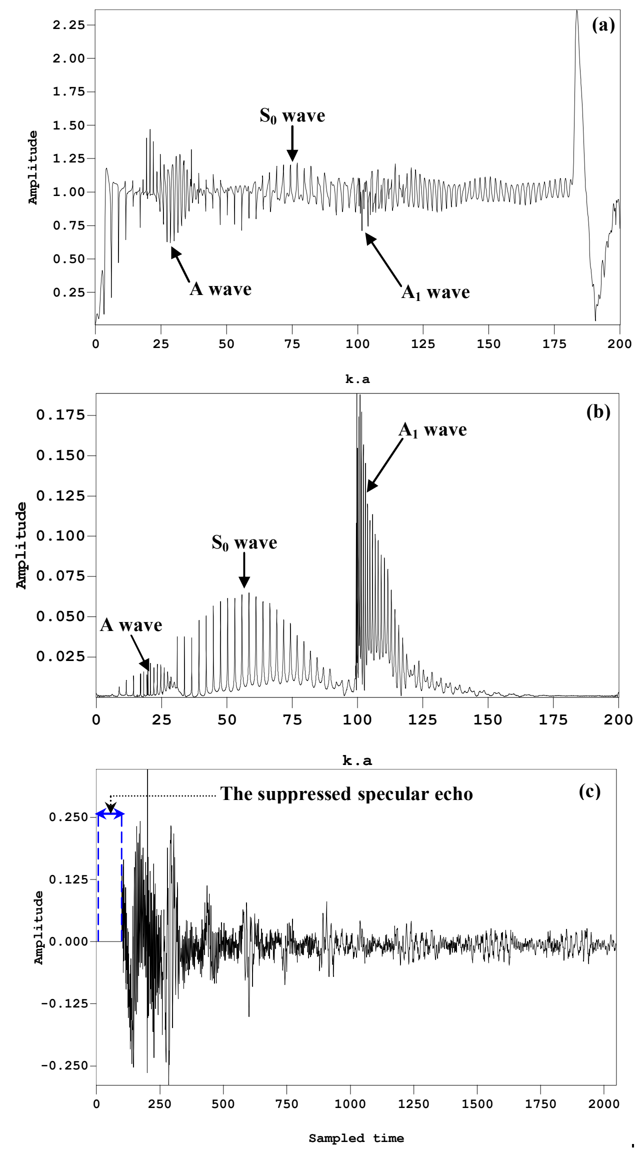

Fig.2 (a) Backscattered spectrum, (b) Resonance spectrum and (c) real part of the temporal signal for an air-filled stainless copper cylindrical schell immersed in water for a radius ratio b/a=0.95.

The backscattered and the resonance spectrums are calculated in the range frequency between 0 and 200. On figures 2a and 2b, we visualize the different circumferential waves such as the scholte wave A ($0<k.a<40$), the symmetrical wave S_0 ($50<ka<100$) and the anti-symmetric wave A_1 ($100<k.a<175$).

3 Time-frequency analysis of the acoustic signal

3.1 Spectrogram

The Short Time Fourier Transform (STFT) can be interpreted as a Fourier analysis of successive sections of the signal weighted by a temporal window (Gabor, Hamming, Blackman...). The expression of the STFT is [1,2,7]:

$$STFT(t,\upsilon)=\int_{-\infty}^{+\infty} x(\tau)h^*_{t,\upsilon}(\tau)d\tau=\int_{-\infty}^{+\infty} x(\tau)h^*(\tau-t)e^{-2\pi j\upsilon\tau}d\tau \quad (3)$$

This relation represents the scalar product between the signal *x(t)* and the functions $h_{t,\upsilon}(\tau)$. In practice, the Spectrogram (SP) is the module square of the STFT and is given by:

$$S(t,\upsilon)=\left|STFT(t,\upsilon)\right|^2 \quad (4)$$

3.2 Wavelet Transform

To make up the deficit of the STFT [2,15], the window size of analysis was varied for better adapting to the different frequencies contained in the signal with an appropriate temporal resolution. It is precisely what is carried out by the wavelet transform (WT). It also based on the projection method of a signal on a family functions. The corresponding family of wavelets consists of a series of son wavelets, which are generated by dilation and translation from the mother wavelet $\psi(t)$, is shown as follows [16]:

$$\psi_{a,b}(t)=\frac{1}{\sqrt{a}}\psi\left(\frac{t-b}{a}\right) \quad (5)$$

where a is the scale factor, b is the time location and $\frac{1}{\sqrt{a}}$ is used to ensure energy preservation.

The higher-frequency and the lower-frequency components can be analyzed if a value is small and a value is larger respectively. The wavelet transform of the signal *x(t)* is defined as follows [16]:

$$WT_x(a,b)=\int_{-\infty}^{+\infty} x(t)\psi^*_{a,b}(t)dt \quad (6)$$

The calculation of the wavelet transform require that the mother wavelet must satisfy the following conditions [4,5,14]:

1. continuous, absolutely integrable and the space of square integrable (finite energy)
2. zero average

$$\int_{-\infty}^{+\infty} \psi(t)dt = 0 \quad (7)$$

3. admissibility condition

$$\int_{-\infty}^{+\infty} \frac{\left|\hat{\psi}\ (\omega)\right|^2}{\omega} d\,\omega < \infty \qquad (8)$$

where $\hat{\psi}(\omega)$ is the Fourier transform of mother wavelet.

In the case of the continuous wavelet transform, *a* and *b* vary continuously. It is the continuous Morlet wavelet which is implemented during this study, defined as follows [6]:

$$\psi(t) = (\pi\sigma_0)^{\frac{-1}{4}} e^{(-\frac{t^2}{2\sigma_0^2})} e^{(-i\omega_0 t)} \qquad (9)$$

ω_0 is the frequency characteristic and σ_0 is the width of the analyzing envelope of the Morlet wavelet.

3.3 Wigner-Ville Distribution

The Wigner-Ville distribution (WVD) associated to a signal *x(t)*, of finite energy, is the function $W_{x_a}(t,v)$ depending on the temporal *t* and frequential ν parameters. This distribution is given by the following expression [5-12]:

$$W_{x_a}(t,\nu) = \int_{-\infty}^{+\infty} x_a(t+\frac{\tau}{2}) x_a^*(t-\frac{\tau}{2}) e^{-j2\pi\nu\tau} d\tau \qquad (10)$$

Where $x_a*(t)$ indicates the complex conjugate of $x_a(t)$.

To avoid covering frequential components in the time-frequency representation, we propose to instead the analytical signal $x_a(t)$, defined by the expression:

$$x_a(t) = x(t) + iH\{x(t)\} \qquad (11)$$

where $i^2=-1$ and $H\{x(t)\}$ is Hilbert transform of *x(t)*.

The spectrum of the analytical function $x_a(t)$ is given below:

$$X_a(k) = \begin{cases} 2X_a & 0 < k < N/2 \\ X_a & k = 0,\ N/2 \\ 0 & N/2 < k < N \end{cases} \qquad (12)$$

3.4 Time-frequency images

The time-frequency images obtained by application of the spectrogram, the Wigner-Wille distribution and the wavelet transform on an acoustic signal backscattered by a copper tube with a radius ratio b/a = 0.95 (Fig.2c). Their time-frequency images are represented on the figure 3 respectively.

4 Comparison between the three time-frequency representations

The spectrogram permits an uniform resolution in time and frequency which is the result of the regular paving of time-frequency space. The wavelet transform uses a different paving. This paving means the fact that the product of the temporal resolution by the frequential resolution is constant on all the scale factors. The wavelet transform gives a better resolution in time for the high frequencies which correspond to fast variations and also gives a lower temporal resolution for the low frequencies which correspond to slow variations.

The Wigner-Ville Distribution presents interference terms between the different trajectory waves. These interferences appear in the form of oscillating structures presenting positive and negative values and decrease the legibility of time-frequency representation. In spite of this disadvantage, the principal advantage of this distribution is that it presents other very interesting properties. Moreover, it preserves the temporal and frequential supports of the signal.

5 Identification of the circumferential waves starting from time-frequency images

Figures 3*a*, 3*b*, 3c and 3d represent the time-frequency images obtained by the spectrogram, the Morlet wavelet transform and the Wigner-Ville distribution. On these images, only trajectories related to the Scholte wave *A* (*0< ka < 40*), with the symmetrical wave *S0* (*50< ka< 100*) and with the antisymmetric wave *A1* (*100< ka < 175*) are present. The trajectories related to the wave *S0* are slightly downward what means that the group velocity of this wave decreases when the frequency increase. The reduced cut-off frequency of the wave *A1* is about of $(ka)_c^{A_1}$ □ 100. It is noted that for the antisymmetric wave *A1* the low frequency part of this wave arrives more tardily than the high frequency part. The reduced cutoff frequency determined starting from this image agrees well with that determined from the proper modes method [13,12].

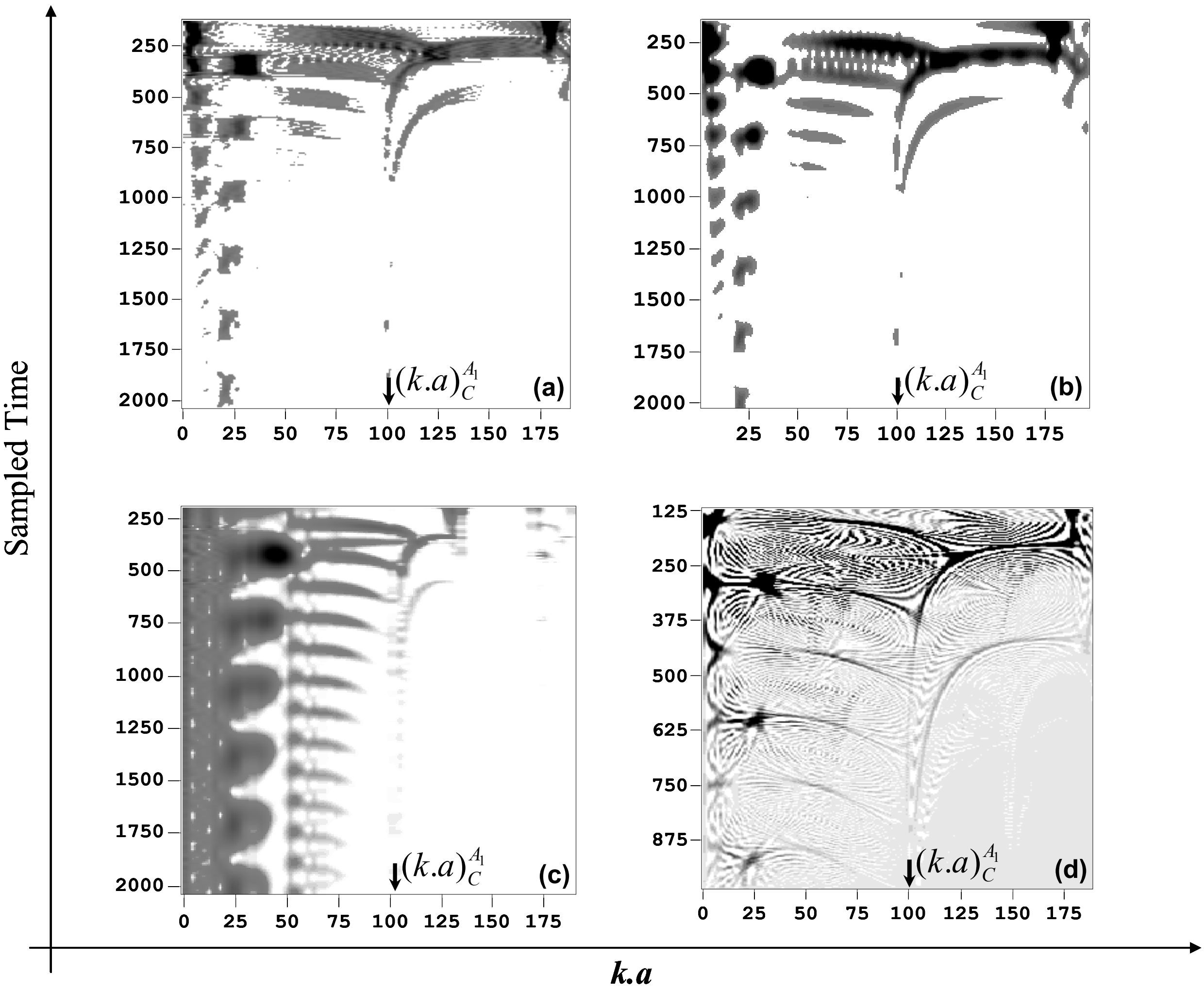

.Fig.3 Time -frequency images: (a) Spectrogram (Gaussian window h=256), (b) Spectrogram (Blackman window h=200), (c) Morlet wavelet transform and (d) Wigner-Ville (Hanning window: temporal smoothing h=256 points and frequential smoothing g=3 points)

6 Determination of the reduced cut-off frequency of the A_1 wave

Starting from the similitude which exists between the circumferential waves in the case of a thin tube and the Lamb waves in the case of the plate of the same thickness, it is possible to use the classical relations on the Lamb waves to ascend to the value of the reduced cut-off frequency of circumferential waves in the case of a tube [8].

In the case of a thin plate the cut-off frequencies of the anti-symmetric waves of Lamb is provided by:

$$(\nu d)_c = \begin{cases} mc_L \\ (m+\frac{1}{2})c_T \end{cases} \qquad (13)$$

Where c_L, c_T are longitudinal and the transverse velocities of a copper tube, d=a-b is the tube thickness and m is the mode number (integer). With c_L= 4760 m/s, c_T = 2325 m/s for a copper tube [8,17].

The reduced cut-off frequency is obtained as a function of the longitudinal and the transverse velocities by exploiting the Eq.(2) and Eq.(13):

$$(ka)_c = \frac{2\pi}{c_1(1-\frac{b}{a})} \begin{cases} mc_L \\ (m+\frac{1}{2})c_T \end{cases} \qquad (14)$$

The values of the reduced cut-off frequencies $(k.a)_c^{A_1}$ of the anti-symmetric circumferential wave A_1 obtained from the time-frequency representations (spectrogram, Wavelet transform and Wigner-Ville : Fig.3) are presented in tabe 1.

	Proper modes theory	Time-frequency images		
		SP	WT	WVD
$(k.a)_c^{A_1}$	99,5	100	101	99,8

Table 1 Reduced cut-off frequencies of the circumferential wave A_1 of a copper tube with b/a=0.95

This table presents also the values computed with the proper modes theory Eq.(14). We notice that the reduced cut-off frequencies estimated from the synthetic time-frequency images are in good concordance with those computed theoretically.

7 Conclusion

The time-frequency images analysis of the spectrogram, the Wigner-Ville distribution and the wavelet transform of an acoustic signal backscattered by a copper tube with the radius ratii b/a=0.95 allowed to visualize and identify the trajectories of the circumferential waves *S0* and *A1*. These images show that the circumferential waves are dispersive. Moreover, starting from these time-frequency representations, it is possible to reach several qualitative and quantitative informations of the circumferential waves. Among qualitative informations one announces that on the time-frequency images, it is possible to follow the evolution of the frequential contents of the circumferential waves *S0* and *A1* versus the time. The dispersion the group velocity of these waves and the reduced cut-off frequency of A_1 are quantitative information which can be given starting from one time-frequency image.

References

[1] S. Qian, D. Chen, "Joint Time-Frequency Analysis" , Prentice Hall, New Jersey (1998)

[2] P. Flandrin, "Représentations temps-fréquence", Ed. Hermes, Paris (1993)

[3] L. Cohen, "Time-frequency analysis", Prentice Hall, New Jersey (1995)

[4] S. Mallat, "A Wavelet Tour of signal processing", Academic Press (1998)

[5] A. Theolis, "Computational Signal Processing with Wavelet", Birkhauser Press, Boston (1998)

[6] S. Qian, "Time-frequency and wavelet transforms", Prentice-Hall Inc., New York, USA (2002)

[7] L. Cohen, "Time-frequency analysis", Prentice-Hall Inc., New York, USA (1995)

[8] R. Latif, E. H. Aassif, G. Maze, D. Decultot, A. Moudden, B. Faiz, "Analysis of the circumferential acoustic waves backscattered by a tube using the time-frequency representation of Wigner-Ville ", Journal of Measurement Science and Technology, Vol. 11 1, pp. 83-88 (2000)

[9] T. Thayaparan, and A. Yasotharan, "Application of Wigner distribution for the detection of accelerating low-altitude aircraft using HF surface-wave radar", Defence Research Establishment Ottawa, DREO TR 2002-033 (2002)

[10] T. Thayaparan, and A. Yasotharan, "A noval approach for the wigner distribution formulation of the optimum detection problem for a discrete-time chirp signal", Defence Research Establishment Ottawa, DREO TR 2001-141(2002)

[11] P. Flandrin, J. Sagéloli, J. P. Sassarego and M. E. Zakharia "Application of time-frequency analysis to the characterization of surface waves on elastic targets", Acoustics letters Vol. 10, n°2, pp 23-28 (1986)

[12] F. Chati, F. Léon, G. Maze . "Acoustic scattering by a metallic tube with a concentric solid polymer cylinder coupled by a thin water layer. Influence of the thickness of the water layer on the two Scholte-Stoneley waves", J Acoust Soc Am. Nov ;118 (5):2820-8 16334660 (2005)

[13] R. Latif, E. Aassif, A. Moudden, B. Faiz, "High resolution time-frequency analysis of an acoustic signal backscattered by a cylindrical shell using a Modified Wigner-Ville representation", Meas. Sci. Technol. 14, , pp. 1063-1067 (2003)

[14] Z. Peng, F. Chu, Y. He, "Vibration signal analysis and feature extraction based on reassigned wavelet scalogram", Journal of Sound and Vibration 253, 1087–1100 (2002)

[15] Jian-Da Wu, Jien-Chen Chen, "Continuous wavelet transform technique for fault signal diagnosis of internal combustion engines" NDT&E International 39, 304–311 (2006)

[16] Jian-Da Wu, Jien-Chen Chen, "Continuous wavelet transform technique for fault signal diagnosis of internal combustion engines" NDT&E International 39, 304–311 (2006)

[17] G. Maze, "Diffusion d'une onde acoustique plane par des cylindres et des tubes immergés dans l'eau. Isolement et identification des résonances", Thèse de Doctorat d'Etat, Rouen (1984)

[18] S. F. Morse and P. L. Marston, "Backscattering of transients by tilted truncated cylindrical shells: Time-frequency identification of ray contributions from measurements", J. Acoust. Soc. Amer., vol. 111, pp. 1289-1294 (2002)

[19] P. L. Marston and N. H. Sun, "Backscattering near the coincidence frequency of a thin cylindrical shell: surface wave properties from elastic theory and an approximate ray synthesis", J. Acoust. Soc. Amer., vol. 97, pp. 777-783 (1995)